MEASUREMENT OF DROPLETS SIZE-TEMPERATURE CORRELATIONS IN SPRAYS WITH COMBINED 3-COLOR LIF AND PDA TECHNIQUES

Alain Delconte [1], Damien Blondel[2], Fabrice Lemoine[1]
[1]LEMTA (CNRS, UMR 7563), 2 avenue de la Forêt de Haye, BP 160,
F-54504 Vandœuvre-lès-Nancy cedex, France, fabrice.lemoine@ensem.inpl-nancy.fr
[2] DANTEC Dynamics, Tonsbakken 16-18, DK-2740 Skovlunde, Danemark,
damien.blondel@dantecdynamics.com

ABSTRACT The present paper is devoted to the development of an optical diagnostic combining 3-color Laser-Induced Fluorescence and Phase Doppler Analyser in order to derive the mean droplet temperature per droplet size class. The PDA is a well-established instrument to measure droplet size and velocity and the three-color LIF technique has been recently developed. The application of this technique in sprays requires taking into account the wavelength dependent scattering of the fluorescence signal. A model based on Beer's extinction was developed and validated. The range of detection of the LIF and PDA techniques, in term of droplet size, is discussed in the light of calculations performed by Generalized Lorentz Mie Theory. The position of the LIF detector is also addressed and two configurations are compared in order to optimize both signal/noise ratio and coincidence rate between LIF and PDA detection. Finally, a demonstration experiment is presented in an ethanol spray injected in an overheated co-flow (air temperature, 100°C), where temperature measurements per droplet size class can be achieved.

List of symbols

a,b temperature sensitivity coefficients [K^{-2}, K^{-1}]
D droplet diameter [m]
$I_{droplet}$ fluorescence intensity emitted by a droplet [$W.m^{-2}$]
I fluorescence intensity sample [$W.m^{-2}$]
I_f fluorescence intensity [$W.m^{-2}$]
I_0 incident excitation intensity [$W.m^{-2}$]
C fluorescent tracer concentration [$mol.l^{-1}$]
T absolute temperature [K]
$R_{ij}=R_i/R_j$ fluorescence ratio
k attenuation per unit of length [m^{-1}]

Greek symbols

λ wavelength [m]

Subscripts

abs absorption
ext extinction
i spectral band
j: droplet index
n sampling index
s droplet size class index
sca scattering

1. Introduction

Heat and mass transfer in sprays is a key problem in the understanding of complex phenomena related to vaporization of liquids in systems using sprays for combustion, freezing, or cooling. In such a process, the droplet size distribution as well as spray concentration must be optimized in order to improve the heat transfers. For example, the average droplet heating time in a combustion chamber or the heat flux extracted by a spray impacting onto a hot surface is strongly linked to the droplet size distribution. In all these situations, heat transfers in the spray can be well characterized by the local liquid phase temperature, which is strongly correlated to the droplet size distribution and concentration. Very few techniques have the potential to provide simultaneously droplet temperature, droplet size distribution and spray concentration. The global rainbow refractometry, introduced by van Beeck et al. (2003) allows measuring the mean droplet temperature of a cloud of droplets concomitantly with droplet size distribution. The present contribution is devoted to the development of an optical diagnostic combining 3-color Laser-Induced Fluorescence and Phase Doppler Analyser in order to determine the mean droplet temperature per droplet size class. The PDA is a well-established instrument to measure droplet size and velocity (Albrecht et al., 2003) and the three-color LIF technique has been recently developed to measure liquid droplet temperature. Three-color LIF requires the use of a fluorescent molecule added to the liquid, which is temperature sensitive. The fluorescence is induced by a suitable laser excitation. Three detection spectral bands are used to measure two fluorescence ratios and therefore to derive the local temperature. The use of three spectral bands allows eliminating the influence of the number of emitting fluorescent molecules, excitation intensity and florescence scattering, making it possible to derive the local temperature. The main principles of multi-band fluorescence will be recalled and the physical modeling of the wavelength dependent fluorescence scattering will be particularly detailed. The same laser source and emission optics are used to induce the fluorescence of the droplets and for the PDA measurements. Both LIF and PDA acquisition systems are synchronized. Two acquisition files (PDA and LIF) are post-processed in order to match the events detected by the two systems and finally the droplet temperature averaged by droplet size class is derived. The range of detection, in term of droplet size, is obviously different for the two techniques, the fluorescence emission being roughly varying as the droplet volume as scattered light for the PDA evolves roughly with the droplet surface. The evolution of the fluorescence emission with the droplet diameter will be quantified with the use of Generalized Lorentz Mie Theory and the effect of the droplet trajectory within the probe volume will be discussed. The position of the LIF and PDA detectors are also addressed and two configurations will be critically compared:

- detection of the LIF signal in the back direction and Mie scattered light, for the PDA measurements, in the forward direction,
- detection of the LIF and Mie scattered light with the same optics in the forward direction.

Finally, a demonstration experiment will be carried out in an ethanol spray injected in an overheated wind tunnel (air temperature, 100°C).

2. Temperature measurements in sprays

2.1. Applications to single droplet: two colors laser-induced fluorescence

The liquid is seeded with a low concentration (a few mg/l) of sulfo-rhodamine B before being disintegrated into droplets. Rhodamine B is an organic dye, used as a fluorescent temperature sensor. Furthermore, the fluorescence of rhodamine B can be easily induced by the green line of the argon ion laser ($\lambda = 514.5$ nm). The rhodamine B fluorescence spectrum is broadband. The fluorescence intensity, collected on a spectral band $[\lambda_{i1};\lambda_{i2}]$, i denoting the spectral band, is given by (Castanet et al., 2003):

$$I_{fi} = \int_{\lambda_1}^{\lambda_2} K_{opt}(\lambda) K_{spec}(\lambda) V_c I_0 C e^{\beta(\lambda)/T} d\lambda \approx K_{opt,i} K_{spec,i} V_c I_0 C f_i(T) \quad (1)$$

where $K_{opt,i}$ is an optical constant taking into account the properties of the detection system (e.g. solid angle of detection and transmission of the optical components), $K_{spec,i}$ is a constant depending solely on the spectroscopic properties of the fluorescent tracer in its solvent, both for the spectral band *i*. I_0 is the laser excitation intensity, C is the molecular concentration of the tracer, T is the absolute temperature, and V_c is the volume from which the fluorescence photons are collected. In fact this volume is the intersection between the laser beam, the droplet and the volume defined by the collecting optics. The product $C.V_c$ is related to the number of fluorescence photons collected by the photodetector. The factor $\beta(\lambda)$ characterizes the temperature dependence of the fluorescence intensity at the wavelength λ (Lavieille et al., 2001). $f_i(T)$ is the function which characterizes the temperature dependence of the fluorescence emitted on the spectral band *i* and can be approximated by (Lavieille et al., 2001):

$$f_i(T) = e^{\frac{a_i}{T} + \frac{b_i}{T^2}} \quad (2)$$

To properly measure the temperature of a moving and potentially evaporating droplet, the influence of the parameters $C.V_c$ and I_0 must be removed. The collection volume V_c is constantly changing as the droplet crosses the probe volume. Furthermore, the distribution of the laser intensity within the droplet depends on the relative position of the droplet in the probe volume and also on the laser beam shape, which is influenced by the refractive and focusing effects of the droplet surface. To eliminate these issues, the fluorescence intensity is detected on two spectral bands for which the temperature sensitivity is highly different. The ratio of the fluorescence intensities collected on the two optimized spectral bands is given by:

$$R_{12} = \frac{I_{f1}}{I_{f2}} = \frac{K_{opt,1}}{K_{opt,2}} \frac{K_{spec,1}}{K_{spec,2}} \frac{f_1(T)}{f_2(T)} \quad (3)$$

This ratio is independent on the dimensions of the probe volume. The influence of the local laser intensity and the tracer concentration are eliminated as well. The use of a single reference measurement at a known temperature eliminates the optical and spectroscopic constants.

2.2. Application to sprays: three colors laser-induced fluorescence

In a spray, we consider now a droplet properly excited by the laser radiation, which emits fluorescence. The fluorescence emission travels through the spray before reaching the detector surface and is therefore affected by wavelength dependent absorption and scattering.
In such a spray, the number of particle $dN(r)$ per unit of volume between the radii r and $r+dr$ is given by:

$$dN(r) = \varphi(r)\, dr \quad (4)$$

where $\varphi(r)$ is the particle concentration distribution function in the direction r (Fig. 1).

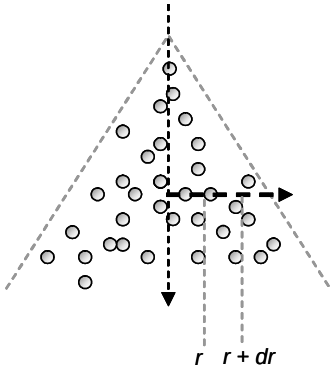

Fig. 1: Sketch of the spray.

The fluorescence attenuation per unit of length within the spray can be written, in a given direction, by:

$$k_{ext,\lambda} = k_{abs,\lambda} + k_{sca,\lambda} = \int_{r=0}^{\infty} C_{abs,\lambda}(r)\varphi(r)\,dr + \int_{r=0}^{\infty} C_{sca,\lambda}(r)\varphi(r)\,dr \tag{5}$$

where $C_{abs,\lambda}$ and $C_{sca,\lambda}$ are respectively the absorption and scattering cross sections of the particle at the radius *r*.

For small particle concentrations and weakly scattering media, the Beer's law can be used (Siegel and Howell, 1983):

$$I_\lambda(z) = I_\lambda(0)e^{-k_{ext,\lambda}Z} \tag{6}$$

where Z corresponds to the geometrical thickness of the medium and I_λ is the local spectral intensity.

Furthermore, it is assumed that the intensity integrated on a spectral band $\Delta\lambda$ can be expressed in the same way:

$$I_{\Delta\lambda}(z) = I_{\Delta\lambda}(0)e^{-k_{ext,\Delta\lambda}Z} \tag{7}$$

where $k_{ext,\Delta\lambda}$ is the attenuation for the spectral band $\Delta\lambda$, depending on the liquid refractive index and spray spatial distribution. In sufficiently dilute sprays and for low dye concentrations, the pure absorption can be neglected (Bruchhausen et al., 2006):

$$k_{ext,\lambda} \approx k_{sca,\lambda} \tag{8}$$

The fluorescence signal integrated on a spectral band *i*, emitted by a droplet in a spray and crossing a geometrical thickness Z in the spray to reach the photodetector, is then determined by:

$$I_{fi} = K_{opt,i}K_{spec,i}V_c I_0 C e^{f_i(T)}e^{-k_{sca,\Delta\lambda i}Z} \tag{9}$$

The closure of the problem requires now having a third equation. A third spectral band of detection, which has the same temperature sensitivity function than the second one (f_2=f_3), will be used. Then, two fluorescence ratios can be written:

$$R_{ij} = \frac{K_{opt,i}K_{spec,i}}{K_{opt,j}K_{spec,j}} e^{-(k_{\Delta\lambda,i}-k_{\Delta\lambda,j})Z} \frac{f_i(T)}{f_j(T)} \qquad \{i=(1,2)\ ;\ (3,2)\} \tag{10}$$

The use of a reference point where R_{ij}, T and Z are known allows removing the system constants $K_{opt,i}$ and $K_{spec,i}$. Then, the two fluorescence ratios can be reformulated by:

$$\ln\left(\frac{R_{12}}{R_{120}}\right) = -(k_{\Delta\lambda 1}-k_{\Delta\lambda 2})(Z-Z_0) + \ln\left(\frac{f_1(T)}{f_2(T)}\frac{f_2(T_0)}{f_1(T_0)}\right)$$

$$\ln(R_{32}/R_{320}) = -(k_{\Delta\lambda 3}-k_{\Delta\lambda 2})(Z-Z_0) \tag{11}$$

where R_{120}, R_{320}, T_0 and Z_0 are the reference quantities.

From the equations set (11), it is possible to derive the quantities $(k_{\Delta\lambda 1}-k_{\Delta\lambda 2})(Z-Z_0)$ and $(k_{\Delta\lambda 3}-k_{\Delta\lambda 2})(Z-Z_0)$ for different operating conditions of the spray (e.g. injection pressures) at a known temperature T.

The plot of $(k_{\Delta\lambda 1}-k_{\Delta\lambda 2})(Z-Z_0)$ against $(k_{\Delta\lambda 3}-k_{\Delta\lambda 2})(Z-Z_0)$ is linear and the slope $\alpha = (k_{\Delta\lambda 1}-k_{\Delta\lambda 2})/(k_{\Delta\lambda 3}-k_{\Delta\lambda 2})$ can be determined regardless to the reference. This relationship is universal for a given fluoresence tracer, liquid and detection spectral bands. An example of this relationship is given in Fig. 2 for water and ethanol seeded with sulfo-rhodamine B. The different points of Fig. 2 correspond to different spray injection pressures, e.g. different optical paths for the fluorescence signal. This kind of calibration must be done one time, for a given optical system, dye and liquid.

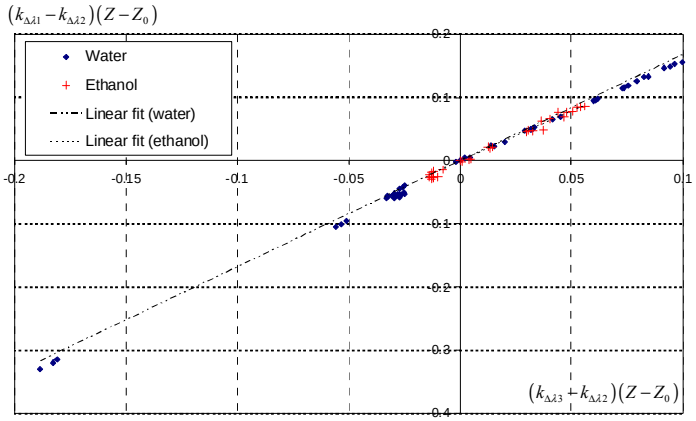

Fig. 2: Evolution of $(k_{\Delta\lambda1}-k_{\Delta\lambda2})(Z-Z_0)$ as a function of $(k_{\Delta\lambda3}-k_{\Delta\lambda2})(Z-Z_0)$ for different spray conditions.

2.3. Measurement process

Two reference fluorescence ratios are measured at a position where the spray temperature can be trustily known by a thermocouple. Then, the fluorescence ratios R_{12} and R_{32} are measured at a current position in the spray.
The ratios R_{32} is used to derive the quantity $(k_{\Delta\lambda1}-k_{\Delta\lambda2})(Z-Z_0)=-\alpha\ln(R_{32}/R_{320})$. Finally, equation (11) can be re-written to derive the local spray temperature:

$$\ln(R_{12}/R_{120})=\alpha\ln(R_{32}/R_{320})+\ln\left(\frac{f_1(T)}{f_2(T)}\frac{f_2(T_0)}{f_1(T_0)}\right) \quad (12)$$

The functions f_1 and f_2 are determined preliminary in a temperature controlled cell.

3. Combined PDA and LIF measurements

3.1. Spray facility

A mechanical atomizer, with spray cone angle of 30°, is supplied by a pressurized liquid tank. The pressure tank and can be varied from $0.5.10^5$ to 6.10^5 Pa in order to modify the spray characteristics such as size distribution and droplet number density. The liquid is ethanol in the present case. A thermocouple is placed just before the nozzle exit to determine the injection temperature T_{inj}. Droplet sizes range typically from 10 µm to 100 µm, with a peak around 35 µm and the velocity at the injection point ranges from 10 to 15 m/s. This spray is injected in a wind tunnel (dimensions and axis are indicated in Fig. 3) equipped with optical accesses. The air in the wind tunnel can be heated up to 150°C by electrical heaters (25kW) and a condenser connected to a drain allows removing the vaporized ethanol from the air.

3.2. Optical set-up

The probe volume is generated by a Laser Doppler Anemometry probe (DANTEC DYNAMICS FiberFlow probe). The probe volume is about 2000 µm long and is 146 µm in diameter (transverse direction). The laser light ($\lambda = 514.5$ nm) scattered by the droplets is high pass filtered and the remaining fluorescence signal is separated into the three spectral bands by means of a set of beamsplitters and interference filters (Fig. 4). The optical signal detection on the three spectral bands is performed by means of three photomultipliers equipped with rapid pre-amplifiers. The

acquisition and sampling of the fluorescence signals are carried out by means of a rapid computerized multi-channel acquisition board. Additionally, a Dual PDA probe (DANTEC DYNAMICS), operating in the refraction mode was used to measure the droplet size distribution in the spray.

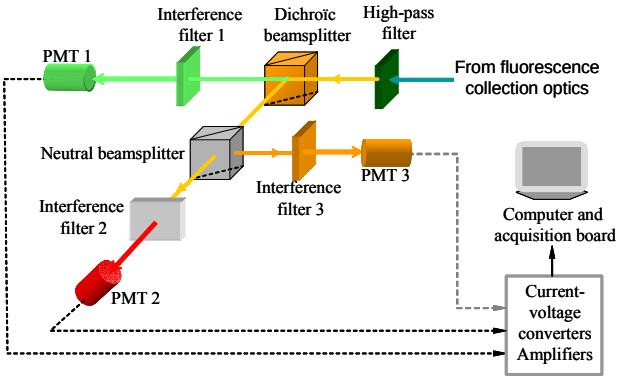

Fig. 4: Three colors LIF optical set-up.

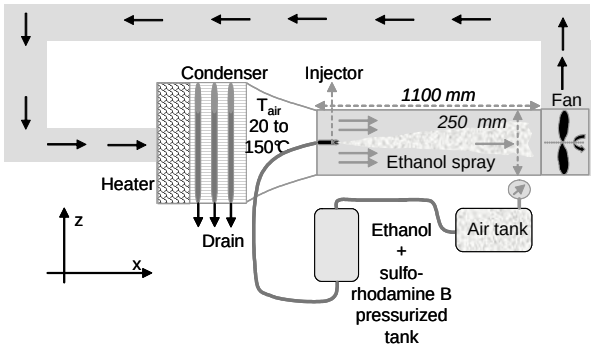

Fig. 3: Experimental facilities.

3.3. Combined LIF and PDA measurement principles

The LIF and PDA acquisition chains are synchronized by using the same reference clock. The two acquisition files (PDA and LIF) are post-processed in order to match the bursts detected by the two systems, using the arrival time criterion. The fluorescence signal emitted by the droplets crossing the probe volume is processed as follows: a detection threshold is fixed above the natural noise level of the photomultipliers. The detected signal I is stored in a buffer and a summation of each sample over the threshold for a given detected droplet, is carried out. The same work is done on the three spectral bands and it is checked that the number of samples, for a given droplet is identical on the three channels. Then, the fluorescence signal $I_{droplet}$ detected for a droplet j on a spectral band i, is given by:

$$\left[I_{droplet} \right]_{ij} = \sum_{n=1}^{k} I_{ni} \tag{13}$$

where i is the spectral band index (i=1, 2 or 3), n is sampling index, j is the droplet index and k is the number of samples on for a given droplet. After identification of the droplets detected by both PDA and three colors LIF system, the fluorescence intensity can be averaged on each droplet size class:

$$I_{fis} = \sum_{j=1}^{N_s} \left[I_{droplet} \right]_{ij} \tag{14}$$

where N_s is the number of droplets in the size class s. Knowing the fluorescence intensities I_{f1s}, I_{f2s} and I_{f3s} per droplet size class, the droplet temperature averaged on the droplet size class s can be calculated using equation (11).

3.4. Fluorescence signal detection

Two detection configurations of the fluorescence signal were tested. On one hand, the LDA probe is connected to a receiving optical fibre acting as a pinhole and allows detecting the fluorescence signal in back-scatter configuration (Fig. 5-a). On the other hand, the DualPDA probe is equipped with four optical apertures: three are used for standard PDA operation and the remaining aperture is used for detecting the fluorescence signal in the same probe volume than the PDA (Fig. 5-b).

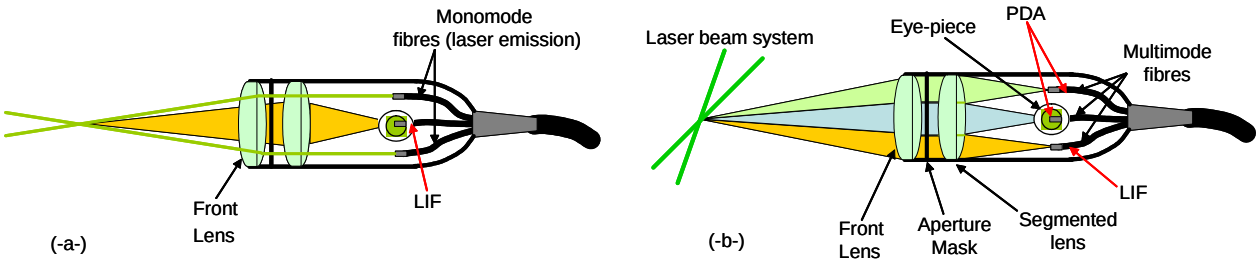

Fig. 5: Fluorescence signal detection strategies.

The first possibility, which consists in detecting the fluorescence in backscatter, exhibits an excellent signal/noise ratio, because the full aperture of the LDA probe front lens is used for the fluorescence detection. However, the fluorescence detection volume is much larger than the one of the PDA, which is limited by the angle between the main axis of the laser volume and receiving probe axis and by the spatial filtering of this probe (slit). This important difference in the probe volume size makes that there is a significant probability to match LIF and PDA events coming from different particles. This phenomenon is obviously likely introducing an important bias in the measurements of the temperature/size correlations. It can be highlighted by measuring the ratio between the number of LIF events matched with a PDA event and the total number of detected LIF events (denoted (LIF+PDA)/LIF). Figure 6 shows for different downstream positions on the spray axis: that this ratio decreases when the spray density decreases, due to the lower occurrence of random coincidences. The second possibility (DualPDA optics) enables to observe similar probe volumes with the same spatial filtering for both fluorescence and PDA techniques. However, the fluorescence signal is much lower compared to the backscatter configuration since the optical system uses a segmented lens, reducing the fluorescence collection aperture by a factor 4. However, the ratio (LIF+PDA)/LIF is much higher for this configuration (around 70% as it was around 10% for the backscatter configuration). Furthermore, this ratio is quite independent on the spray density. Consequently the detection of the fluorescence signal with the use of the DualPDA probe is probably the optimized solution for measuring temperature/size correlations, although the bad signal/noise ratio.

3.4. LIF detection size range

According to equation (1), the fluorescence signal is directly proportional to the droplet volume i.e. should vary as D^3. For the PDA, the scattered light evolves as D^2. In principle, the PDA should have a much larger detection range in term of droplet size, than the LIF technique. The Gaussian distribution of the energy in the laser beam and the focusing effect of the droplet interface lead to a non-uniform distribution of the laser energy within the droplet. Then, the term $V_c I_0 C f_i(T)$ of equation (1) must be rewritten:

$$V_c I_0 C f_i(T) \sim \gamma \int_V Ci(x,y,z)\, f_i\left(T(x,y,z)\right) dxdydz$$

where *i(x,y,z),* is the local density of excitation energy and V the droplet volume as the factor γ represents the fraction of the droplet volume seen by the collection optics ($\gamma \in [0,1]$). The function $f_i(T(x,y,z))$ is spatially constant if the droplet is at thermal equilibrium, i.e. if there are no temperature gradients inside the droplet. The local density of excitation energy *i(x,y,z)* can be evaluated using Generalized Lorentz-Mie Theory (GLMT). The original Lorenz-Mie theory gives a rigorous solution to the problem of interaction between a plane wave and spherical particle. This theory has been extended to the case of partial illumination of the particle with a focused beam (Gouesbet et al., 1988). GLMT is able to quantify rigorously the scattered fields (far and near field),

the internal fields and the radiation pressure forces from a regularly shaped particle illuminated by an arbitrary shaped beam. An overview of GLMT principles and applications can be found in the literature (Gouesbet and Grehan, 2000; Mees et al., 2001). A computation code, based on GLMT, has been developed by the CORIA laboratory (Rouen; France), specially adapted for a LDV laser beams system. The computation input parameters are:

- liquid refractive index information (supposed constant)
- laser beam diameter in the focus point of the front lens of the LDV system
- position (x, y, z) of the droplet centre according to the beam axis intersection
- wavelength of the laser radiation
- beam angle (in the case of a LDV beams system)
- polarization direction of the incident laser beams

The code output is a 3D excitation field. The evolution of the term $\int_V i(x,y,z)dxdydz$ calculated by GLMT is represented in Fig. 7 as a function of the droplet diameter, in comparison with the cubic evolution of the intensity, in the case of the droplets centred in the probe volume. It appears clearly that the intensity of fluorescence emitted by a droplet evolves slower than D^3. Furthermore, the fluorescence intensity depends on the trajectory of the droplet in the probe volume, due to the non-uniform distribution of the laser energy and the possible interaction of a limited part of the droplet with the laser excitation volume. This trajectory effect can benefit to the fluorescence detection because it extends the size range which can be investigated by a fluorescence technique. As seen on the example of Fig. 8, a big particle having an off-centered trajectory in the probe volume can emit comparable fluorescence intensity than a smaller one. This phenomenon is well summarized in Fig. 9, where the fluorescence intensity, assuming proportionality with the excitation field, calculated by GLMT is presented for variable distance x between the droplet center and probe volume axis (see Fig. 8) and droplet diameters.

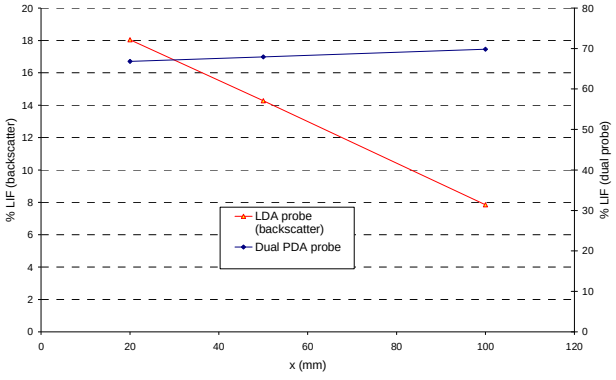

Fig. 6: Downstream evolution of the ratio (LIF+PDA)/LIF.

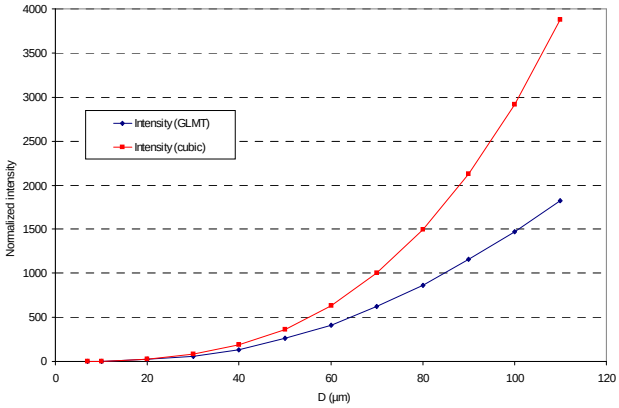

Fig. 7: Fluorescence emission of a droplet (centered in the probe volume) as a function of the droplet diameter.

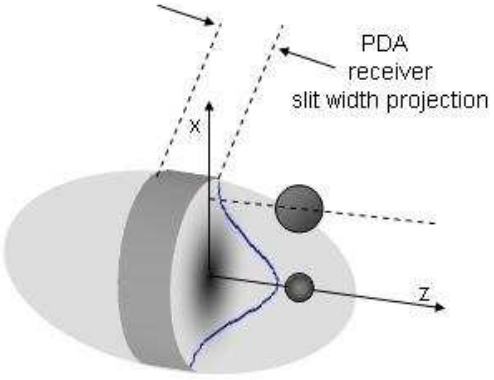

Fig. 8: Trajectory effect for the fluorescence signal.

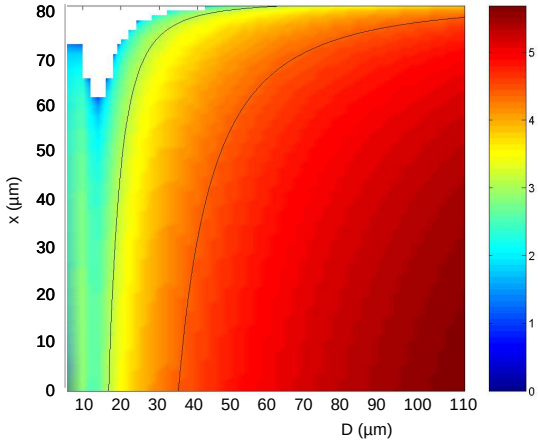

Fig. 9: Fluorescence emission of a droplet as a function of the droplet diameter and distance from the probe volume main axis. Intensity units A. U.?

4. Experimental results

4.1. Preliminary tests

In order to test the performances of the temperature measurement, preliminary tests were performed in a temperature controlled water spray, placed in a vapour saturated enclosure. The detection in backscatter was used. The random error was studied by increasing gradually the number of droplets used in the averaging process (Eq. (13)). The RMS value, calculated on 5 spray temperature measurements decreases when the number of drop increases and is within ± 0.5°C for about 5000 droplets. By taking into account the sources of uncertainties in the calibration process (fluorescence versus temperature, fluorescence scattering) a systematic shift of the measurements in the range ± 1°C can be identified.

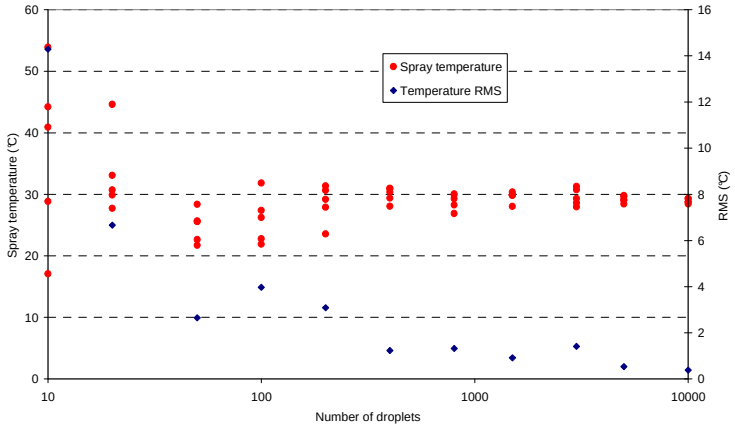

Fig. 10: Influence of the number of droplets involved in the averaging process.

4.2 LIF and PDA detection ranges

The experimental results concerning the ethanol spray (injection temperature is about 48°C) injected in the hot air coflow (velocity V_{air}=6.2 m/s, temperature T_{air}=103°C) are developed in this section. The optics was the DualPDA for both LIF and PDA measurements. The droplet size histograms constructed with the raw PDA data and with data resulting from coincidence between PDA and LIF events were compared at different downstream positions in the spray axis (Fig. 11). The PDA histograms include about 280.10^3 droplets and the combined LIF and PDA data histograms include

about 27.10^3 droplets. Because of the evaporation, the raw data histograms exhibit a progressive shift toward bigger droplet sizes as well as a noticeable decrease in the population of the smallest droplets, for increasing downstream distances. Close to the nozzle exit (e.g. x=20 mm), the histogram corresponding to the coincident LIF and PDA data is clearly shifted to the biggest droplet sizes, because the major part of fluorescence coming from the smallest droplets cannot be detected by the LIF technique. This shift tends to vanish for increasing downstream distances, i.e. when the smallest droplets evaporate and the two histograms become almost similar at x=150 mm. The PMT high voltages of the LIF detection chain are adjusted so as the maximum number of droplets around x=30 mm reaches the maximum detectable intensity, i.e. for the droplets with a size of about 35 µm. It means that some of the biggest droplets may saturate the detectors and are therefore rejected from the subsequent processing. Taking into account the signal/noise ratio of the fluorescence detection chain (PMT + pre-amplifier), the fluorescence signal detection range extends from a factor 1 to 20. If the intensity emitted by a 35µm-diameter droplet, centered in the probe volume is considered as the maximum detectable signal, it is possible to estimate roughly detection range of the LIF technique as a function of droplet size and distance from the probe volume axis, using the preliminary GLMT calculations (Fig. 9). As seen in Fig. 9, it is possible to capture droplets from 17 µm in diameter with centered trajectories, as the biggest droplets can also be seen up to 100 µm in diameter but with off-centered trajectories. The presence of droplets detected by the LIF chain under the size 17 µm is probably due to the coincidence of two droplets in the probe volume which causes a summation of each fluorescence intensities. This phenomenon occurs in the denser zone of the spray, close to the nozzle exit. The Sauter mean diameter (SMD) plotted in Fig. 12, as a function of the downstream distance, presents very similar trends when calculated with the use of the PDA data and coincident data. The SMD increases after x=40 mm due to evaporation as the decrease in the initial zone can be explained by erroneous measurements of both instruments (e.g. occurrence of the presence of two particles in the probe volume), due to the high density of the spray in the vicinity of the nozzle exit.

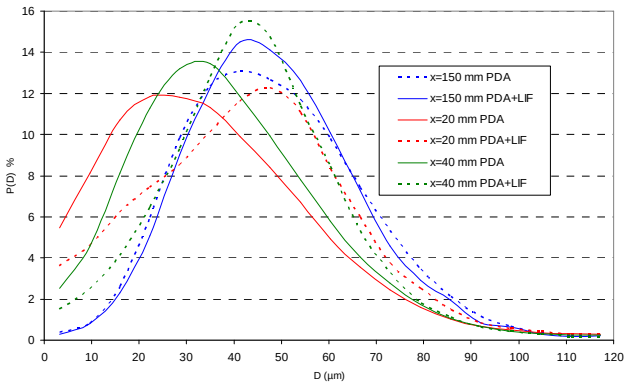

Fig. 11: Droplet size histograms constructed with the raw PDA data and with data resulting from coincidence between PDA and LIF events, at different downstream positions in the spray.

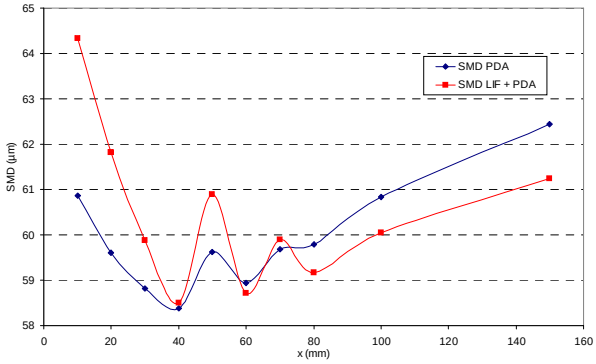

Fig.12: Downstream evolution of the SMD.

4.2. Size-temperature correlations

The evolution of the droplet mean temperature as well as the droplet temperature evolution per droplet size class is presented in Fig. 13 at different positions on the spray axis. The mean droplet temperature measured in the transverse direction at x=50 mm and x=70 mm are also reported. In a first phase, the spray temperature decreases due to the strong vaporization at this injection temperature and tends to stabilize when equilibrium between heat fluxes exchanged by forced convection and vaporization is reached. The number of droplets per size class varies from 900 (diameter class 8 µm) to 3000 (diameter class 72 µm). The radial exploration of the spray, far from the injection nozzle, exhibits

a quite homogeneous temperature distribution, probably related to the good turbulent mixing of the spray with the hot air flow. It is, in the present form, difficult to distinguish any clear trend concerning the temperature evolution for each droplet size class. A clearer trend appears in the plot of the temperature evolution as a function of the size class for different radial positions in the spray at x=50 mm and x=70 mm (Fig. 14). The biggest droplets seem to be colder of a few degrees than the smallest which is well correlated to heat diffusion within the droplets. As similar trend is observable for each of the explored radial positions at x=50 mm and x=70 mm. These plots are slightly scrambled because of the low signal/noise ratio obtained with the use of the DualPDA probe and because of the limited number of droplets in each size class. The number of droplets per size class was also reported in Fig. 14 (for the position z=0), leading to an expected accuracy within ± 1°C (see Fig. 10), according to the number of droplet per size class, which is compatible with the experienced accuracy.

6. Conclusions

The combination of the three colors laser-induced fluorescence and Phase Doppler Anylizer techniques for droplet temperature, size and velocity in a liquid polydisperse sprays has been investigated. The wavelength dependent attenuation of the fluorescence emission due to scattering has been taken into account using a simple Beer model. The detection range of the LIF technique has been investigated using calculations of the droplet internal excitation field. This range can be considerably improved by optimizing the signal/noise ratio of the LIF detection chain.
Combined LIF and PDA measurements have been carried out. Such combination constitutes certainly a new investigation tools for a deaper comprehension of complex phenomena involving heat and mass transfers in sprays and for the validation of the numerical models.

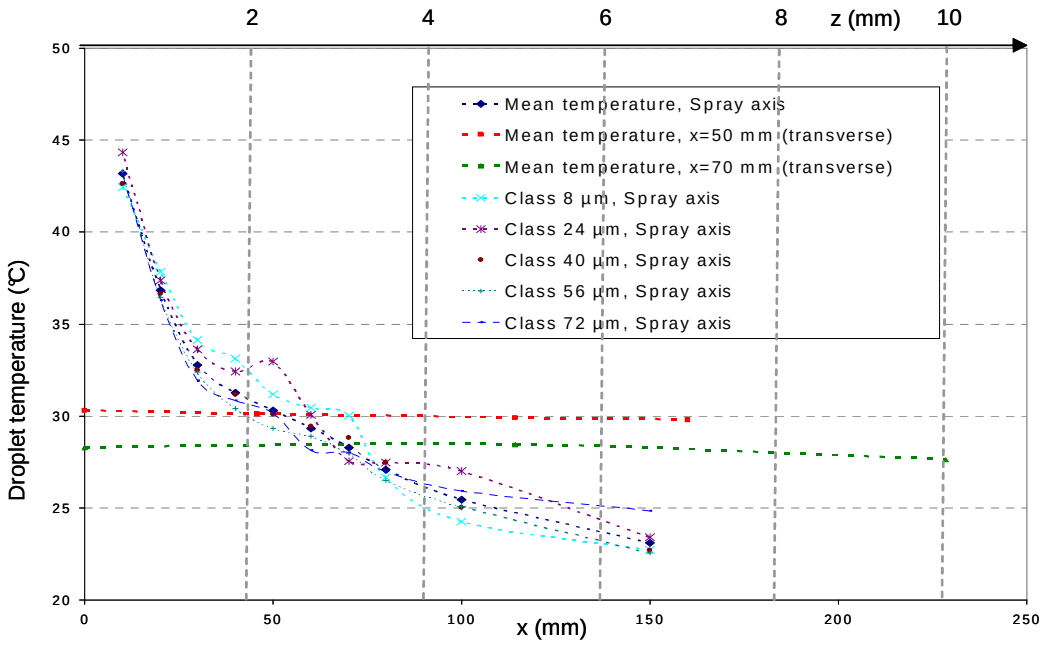

Fig. 13: Downstream evolution of the droplet temperature per droplet size class.

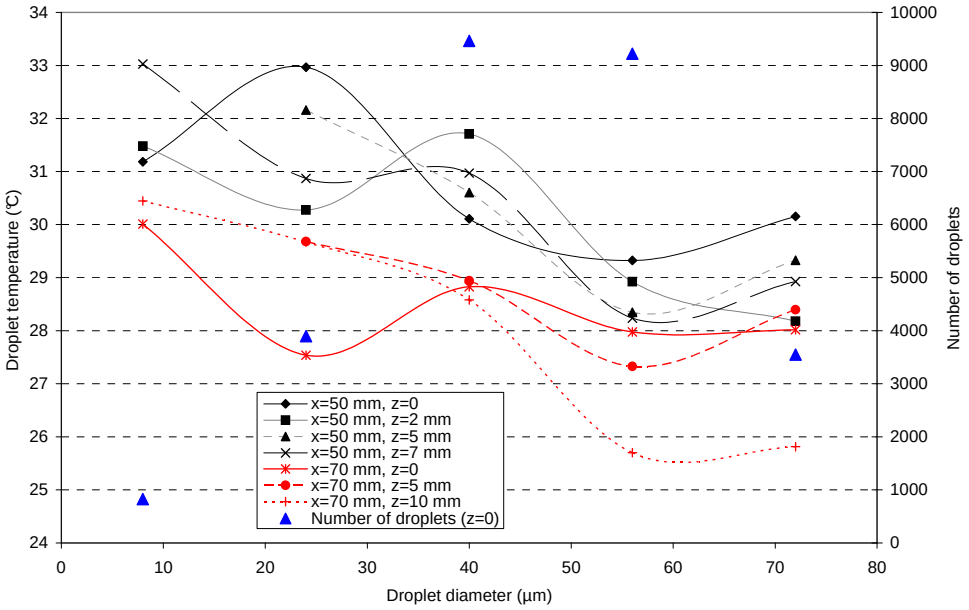

Fig. 14: Evolution of the droplet temperature as a function of the droplet diameter for different radial positions.

Aknowledgment

The authors wish to thank Loic Mees and Gérard Gréhan for their help in the implementation of the GLMT calculations.

References

Albrecht H.-E, Borys M, Damaschke N, Tropea C, Laser Doppler snd Phase Doppler Measurement Techniques. Springer editor. 2003.

Bruchhausen M, Delconte A, Blondel D, Lemoine F (2006) Temperature Measurements in Polydisperse Sprays by means of Laser-Induced Fluorescence (LIF) on Three Spectral Bands, Atomization and Sprays, under press: to appear.

Castanet G, Lavieille P, Lebouché M, Lemoine F (2003) Measurement of the temperature distribution within monodisperse combusting droplets in linear stream using two colors laser-induced fluorescence, Exp. in Fluids 35: 563-571.

Gouesbet G, Gréhan G (2000) Generalized Lorenz-Mie Theories, from past to future, Atomization and Sprays 10: 277-333.

Gouesbet G, Maheu B, Gréhan G (1988) Light scattering from a sphere arbitrarily located in a Gaussian beam, using a Bromwich formulation, J. Opt. Soc. Am. A5: 1427-1443.

Lavieille P, Lemoine F, Lavergne G, Lebouché M (2001) Evaporating and combusting droplet temperature measurements using two-color laser-induced fluorescence, Exp. in Fluids 31: 45-55.

Mees L, Gouesbet G, Gréhan G (2001) Interaction between femtosecond pulses and a spherical microcavity : internal fields., Optics communications 199: 33-38.

Siegel R, Howell JR (1983) Thermal Radiation Heat Transfer, 3rd ed., Hemisphere Publishing Corp., New York.

van Beeck JPAJ., Grosges T, De Giorgi MG (2003) Global rainbow thermometry assessed by Airy an Lorentz-Mie theories compared with Phase Doppler anemometry, Applied Optics 42(19): 4016-4022.